

The Role of the Electron Tunneling Effect in the Coagulation Kinetics of Polydisperse Metal Nanocolloids

S. V. Karpov^{a, b}, P. N. Semina^a, and A. P. Gavriluk^c

^a Kirensky Institute of Physics, Siberian Branch, Russian Academy of Sciences, Akademgorodok, Krasnoyarsk, 660036 Russia

^b Siberian Federal University, ul. Kirenskogo 26, Krasnoyarsk, 660028 Russia

^c Institute of Computational Modeling, Siberian Branch, Russian Academy of Sciences, Akademgorodok, Krasnoyarsk, 660036 Russia

e-mail: karpov@iph.krasn.ru

Received June 24, 2011

Abstract—The energy of pair interactions between metal nanoparticles of different sizes is shown to be able to increase upon coagulation due to the additional electrostatic effect resulting from mutual heteropolar charging of the particles. The tunnel electron transfer occurring upon the collisions between particles of different sizes may be the reason for the charging. The transfer is caused by the dependence of the electron work function on the particle size. The electron transfer through the interparticle gap equalizes the Fermi levels in particles of different sizes and is associated with this dependence. Using the example of bimodal silver nanocolloids, it is shown that mutual heteropolar charging of particles with different sizes may accelerate the coagulation of polydisperse colloidal systems by an order of magnitude or more as compared with monodisperse systems, in which this effect is absent.

DOI: 10.1134/S1061933X12030052

1. INTRODUCTION

In our previous study [1], the coagulation kinetics of metal nanocolloids with different degrees of polydispersity was analyzed using the Brownian dynamics method. It was found that the results obtained contradict the conclusion of the Muller–Smoluchowski theory that the coagulation of nanocolloids accelerates with an increase in the degree of their polydispersity [2]. This contradiction can be observed at a low viscosity of a dispersion medium, upon stabilization of nanoparticles with adsorption layers (ALs), and when both of the factors are combined; simulation by the Brownian dynamics method did not exhibit the accelerated coagulation predicted by the theory.

Nevertheless, a number of experiments on the coagulation kinetics of polydisperse metal colloids attest to accelerated coagulation in systems containing particles with greatly different sizes [2–5].

According to the existing ideas [6–8], a polydisperse ensemble composed of metal nanoparticles reaches the thermodynamic equilibrium, provided that the electrochemical potentials of electrons in the particles are equalized due to their exchange through an electroneutral interparticle medium. The electron tunneling effect (ETE), which is observed upon accidental collisions between particles of different sizes and their interaction through thin (less than 1 nm) polymer ALs, may be one of the ways of this exchange. The equilibrium interparticle gap at the moment of interparticle collision at a corresponding AL thickness

must be no larger than 1–1.2 nm, which is sufficient for a noticeable tunneling current [9]. It was demonstrated that the ETE can result in mutual heteropolar charging of particles with different sizes at the moment of their collision [9]. The predominant electron transfer from one particle to another is conditioned by the dependence of the electron work function on particle size; the transfer promotes equalization of the Fermi levels in particles of different sizes. As a result of this exchange, one particle acquires a positive charge, whereas the other becomes negatively charged to induce electrostatic attraction in addition to the Van der Waals interaction.

Quantum-size corrections to the work function of particles with different sizes in a silver nanocolloid, which ensure the mutual heteropolar charging of the particles, were taken into account, and the electrostatic effects accompanying the interaction between charged particles were analyzed and taken into account in this study. As opposed to [9], a dynamic approach to the description of the mutual heteropolar charging of particles upon their collisions and disintegration of particle aggregates was implemented in this study. Furthermore, the effect of this process on the particle coagulation kinetics was assessed.

The possibility of the realization of the ETE, which causes an additional electrostatic interaction between nanosized particles, was demonstrated in [9]. The ETE made it possible to clearly explain the experimental results reported in [10, 11], where the forma-

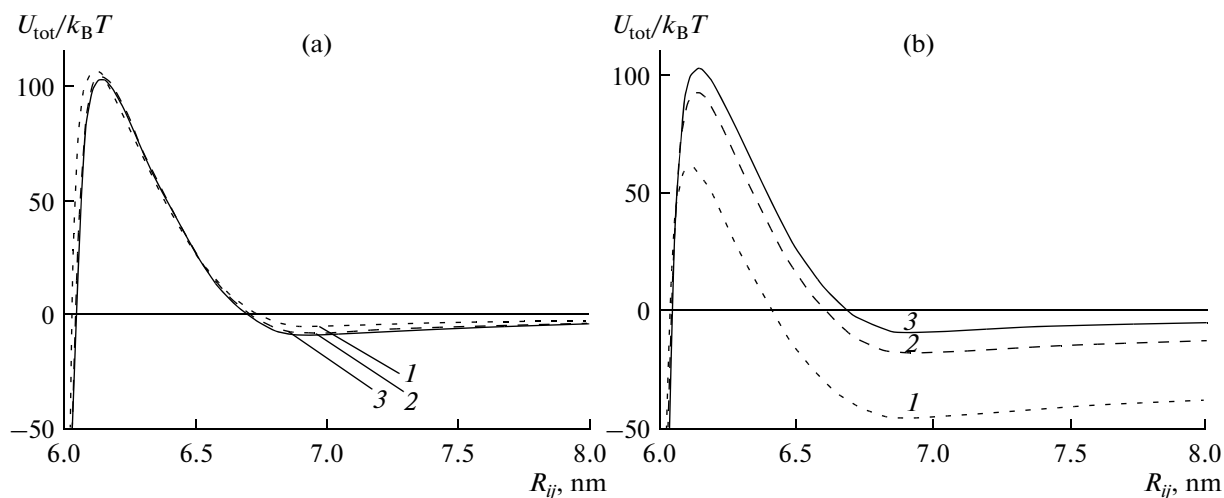


Fig. 1. Pair potential dependences of the total interparticle interaction ((a) Van der Waals and elastic and (b) Van der Waals, elastic, and Coulomb) for a pair of particles with radii (1) $R_i = 1$ and $R_j = 5$, (2) $R_i = 2$ and $R_j = 4$, and (3) $R_i = R_j = 3$ nm. Thickness of the polymer AL for all of the pairs is $h_i = h_j = 0.5$ nm. The elasticity modulus of AL is $E_e = 3 \times 10^9$ N/m². The charge value for the pair $R_i = 1$ and $R_j = 5$ nm is $\pm 20e$ and, for the pair $R_i = 2$ and $R_j = 4$ nm, it is $\pm 10e$ (e is the elementary charge, k_B is Boltzmann's constant, $T = 300$ K).

tion of two-dimensional superlattices in bimodal gold organosols was investigated. The superlattices consisted of hexagonal sublattices formed from monodisperse particles with a certain size ratio, with the sublattices being enclosed into one another. This crystal lattice geometry cannot be explained using the Van der Waals and elastic interactions alone; however, it can result from the selective attraction of particles with different sizes.

The possible existence of forces generated by mutual charging in ensembles of small particles and the experimental data on the dependence of the work function on the size of a spherical particle were discussed in, e.g., [6–8]. Note that the electron transfer via tunneling between metal particles forming ordered monolayer films was investigated in a large number of studies (see review [12]).

The goal of this work was to employ the Brownian dynamics method for studying the effect of ETE on coagulation of polydisperse metal nanocolloids with allowance for realistic models of interparticle interactions and dissipative forces.

2. MODEL

2.1. Electron Tunneling Effect and Mutual Heteropolar Charging of Particles of Different Sizes

The development of electrostatic attraction, in addition to the Van der Waals interactions in an ensemble of polydisperse particles, is accompanied by an increase in the coagulation efficiency of collisions between particles of different sizes. The depth of the secondary potential well in the potential energy of pair interparticle interaction is markedly enlarged as compared with that for particles of the same size (Fig. 1)

due to the additional attraction between the particles of different sizes, and this phenomenon affects the rate of coagulation.

The possibility of tunnel electron exchange, resulting in the heteropolar charging of particles, is determined by a small distance (~ 1 nm) between particle surfaces at the moment of their collision.

In the general case, the coefficient of electron tunneling from particle i with radius R_i and energy $W(R_i)$ through potential barrier $W_0(x)$ of an arbitrary shape is determined by the following expression [13]:

$$D = C \exp \left[-\frac{2}{\hbar} \sqrt{2m} \int_{\tilde{x}_0}^{\tilde{x}_1} \sqrt{W_0(x) - W(R_i)} dx \right], \quad (1)$$

where $C \approx 1$ is a constant.

In the simplest case of a rectangular barrier with width L , the expressions for coefficients j , D_{ij} of electron tunneling from particle i to particle D_j and in the opposite direction are written as:

$$\begin{aligned} D_{ij} &= \exp \left[-\frac{2}{\hbar} \sqrt{2m(W_0(x) - W_F(R_i))L} \right], \\ D_{ji} &= \exp \left[-\frac{2}{\hbar} \sqrt{2m(W_0(x) - W_F(R_j))L} \right], \end{aligned} \quad (2)$$

where W_0 is the potential barrier height and W_F is the Fermi level in particle i or j (in our case, L corresponds to h equal to the sum of the thicknesses of deformed adsorption layers on the particles in the contact zone).

Variation in the work function with particle size R_i is determined by the following factors [8]:

$$W(R_i) = |W_0 - W_F(R_i)| \quad (3)$$

$$= W_{\text{bulk}} - \Delta W_{\text{bulk}}(R_i) - \Delta W_F(R_i) - W_{\text{im,em}}.$$

The physical meanings of the characteristics introduced into Eq. (3) are as follows: W_{bulk} is the work function for a bulk metal and $\Delta W_{\text{bulk}}(R_i) = \frac{5e^2}{32\pi\epsilon\epsilon_0 R_i}$ is the size correction to the work function in case of a spherical particle with radius R_i [14], where ϵ is the permittivity of an environment, ϵ_0 is the permittivity of vacuum, and e is the elementary charge. In the approximation of perfectly spherical particles, the dimensional correction to the Fermi energy $\Delta W_F(R_i)$ is described as [8, 15]

$$\Delta W_F(R_i) = W_F(R_i) - W_{\text{bulk}} \cong \frac{\pi W_{\text{bulk}} S_i}{4k_F V_i}, \quad (4)$$

where $W_F = \frac{\hbar^2(3^2 n_e)^{2/3}}{2m}$ is the Fermi energy of a bulk metal; R_i , S_i , and V_i are the radius, surface area, and volume of a particle, respectively; n_e is the electron concentration in a particle; m is the effective mass of the electrons; and k_F is the Fermi wave number.

The fourth term, $W_{\text{im,em}} = e\phi_i$, is the additional electrostatic attraction, which is responsible for an increase in the electrostatic potential of an emitting particle in the field of an oppositely charged neighboring particle [16]. Actually, this term reflects the potential energy of an emitted electron in the field of the two particles. It is expressed via the charges of the emitting q_i and neighboring q_j particles,

$$\phi_i = \frac{c_{ij}q_i - c_{ij}q_j}{c_{ii}c_{jj} - c_{ij}^2} \quad (5)$$

and the capacitance coefficients c_{ij} , which are derived using the method of electrical images and written as follows [16]:

$$c_{ii} = 4\pi\epsilon\epsilon_0 R_i \gamma \text{sh}\beta \sum_{n=1}^{\infty} \{\gamma \text{sh}(n\beta) + \text{sh}[(n-1)\beta]\}^{-1},$$

$$c_{ij} = 4\pi\epsilon\epsilon_0 R_i \gamma \frac{\text{sh}\beta}{(1+\gamma)x} \sum_{n=1}^{\infty} \{\text{sh}(n\beta)\}^{-1}, \quad (6)$$

$$c_{jj} = 4\pi\epsilon\epsilon_0 R_j \gamma \text{sh}\beta \sum_{n=1}^{\infty} \{\text{sh}(n\beta) + \gamma \text{sh}[(n-1)\beta]\}^{-1}.$$

In Eqs. (6), $\gamma = R_j/R_i$ and $x = R_{ij}/(R_i + R_j)$, where R_{ij} is the distance between the particle centers. Parameter β is related to the distance between the centers of the nanoparticles as follows:

$$\text{ch}\beta = \frac{x^2(1+\gamma)^2 - (1+\gamma^2)}{2\gamma}. \quad (7)$$

Let us consider the way in which the size and electrostatic corrections to the work function in the Brownian dynamics model may result in the asymmetry of counter electron fluxes between two metal nanoparticles, which, in the long run, leads to mutual charging of particles of different sizes.

Taking into account that electron tunneling occurs through a gap of a variable thickness corresponding to the distance between two spherical surfaces with radii R_i and R_j , the expression for the electron flux from particle i via an elementary ring surface with radius x and surface area $2\pi x dx$ is modified according to the following relationship [9] (x is the coordinate along the axis perpendicular to the intercenter vector, $0 \leq x \leq R_i$, and R_i is the radius of the smaller particle):

$$dn_{ij}(x) = \frac{1}{6} n_e \sqrt{\frac{3}{5}} v_F D_{ij}(x) 2\pi x dx, \quad (8)$$

$$dn_{ji}(x) = \frac{1}{6} n_e \sqrt{\frac{3}{5}} v_F D_{ji}(x) 2\pi x dx,$$

where factor $\sqrt{3/5}$ determines the mean electron velocity related to the electron velocity at the Fermi level, v_F , and factor $1/6$ corresponds to the fraction of electrons moving along the direction of intercenter vector \mathbf{R}_{ij} .

Tunneling coefficients D_{ij} and D_{ji} are determined by expressions

$$D_{ij}(x) = \exp\left[-\frac{2}{\hbar} \sqrt{2mW(R_i)}\right] \times \left[L + \left(R_i - \sqrt{R_i^2 - x^2} \right) + \left(R_j - \sqrt{R_j^2 - x^2} \right) \right], \quad (9)$$

$$D_{ji}(x) = \exp\left[-\frac{2}{\hbar} \sqrt{2mW(R_j)}\right] \times \left[L + \left(R_i - \sqrt{R_i^2 - x^2} \right) + \left(R_j - \sqrt{R_j^2 - x^2} \right) \right],$$

where L is the current width of the interparticle gap.

Then, the numbers of electrons transferred from particle i to particle j during iteration time step Δt are equal to

$$n_{ij}(\Delta t) = \frac{1}{6} n_e \sqrt{\frac{3}{5}} v_F \int_0^{R_i} D_{ij} 2\pi x dx \Delta t, \quad (10)$$

$$n_{ji}(\Delta t) = \frac{1}{6} n_e \sqrt{\frac{3}{5}} v_F \int_0^{R_j} D_{ji} 2\pi x dx \Delta t.$$

The difference between the numbers of electrons transferred during time period Δt is

$$\Delta n(\Delta t) = n_{ij}(\Delta t) - n_{ji}(\Delta t). \quad (11)$$

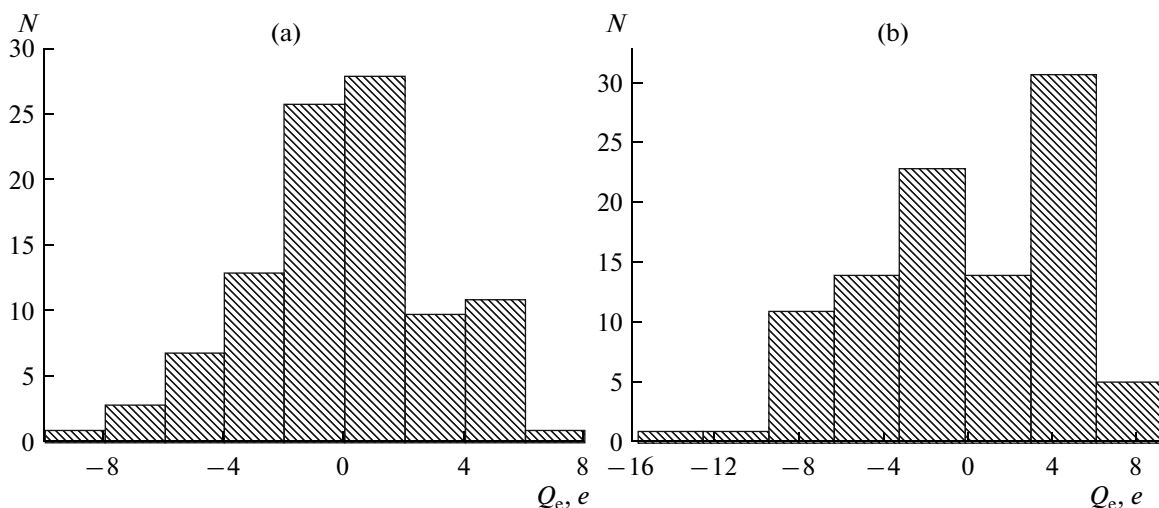


Fig. 2. Histograms of particle charge distribution in ensembles with (a) $R_i = 2$ and $R_j = 4$ and (b) $R_i = 1$ and $R_j = 5$ nm; $h_i = h_j = 0.5$ nm; N is the number of particles in an ensemble, with the particles having charge Q_e in elementary charge units (e).

The charge value at the current iteration step varies according to the calculated number of electrons transferred at this step:

$$\begin{aligned} Z_{i+1} &= Z_i + \Delta Z(\Delta t), & Z_{j+1} &= Z_j - \Delta Z(\Delta t), \\ \Delta Z(\Delta t) &= \Delta n(\Delta t)e. \end{aligned} \quad (12)$$

The equilibrium charge of the particle pair is attained over time t_{eq} ; as this time passes, the electron exchange ceases:

$$Z_i(t_{\text{eq}}) = \sum_{i=0}^N Z_i, \quad Z_j(t_{\text{eq}}) = \sum_{j=0}^N Z_j, \quad N = \frac{t_{\text{eq}}}{\Delta t}. \quad (13)$$

It should be noted that the characteristic time of the establishment of the equilibrium between the charges in a particle pair is longer than the coagulation half-time and is equal to 10^{-7} s, whereas the coagulation half-times are shorter by one or two orders of magnitude depending on the viscosity of an interparticle medium.

During the period corresponding to the coagulation half-time, the average absolute value of the charge of $N = 100$ silver nanoparticles with radii $R_i = 1$ and $R_j = 5$ nm in a bimodal ensemble is equal to $4e$, while that for an ensemble consisting of particles with radii $R_i = 2$ and $R_j = 4$ nm is equal to $1.5e$.

The pattern of particle charge distributions in bimodal ensembles is illustrated by histograms in Fig. 2. It is clear that the range of particle charges is wider for the ensemble with the higher degree of polydispersity. This type of particle charging promotes a considerable increase in the depth of the secondary potential minimum and, therefore, enhances the coagulation efficiency of the collisions.

2.2. The Brownian Dynamics Model with Allowance for the Dynamic Electrostatic Interparticle Interaction

Let us supplement the Brownian dynamics model [1] with allowance for the mutual heteropolar charging of particles of different sizes and the electrostatic interaction thereof (including its short-range component).

The fundamental possibility of ETE upon colloidal crystallization of bimodal gold nanoparticles was demonstrated in [9]. Fixed particle charges, which were assessed using the tunneling coefficients and the times of interparticle diffusion contacts, were considered in that work.

Here, we take into account the dynamic tunnel electron exchange with regard to variations in the charges of colliding particles of different sizes during the time of the contact between their adsorption layers at each iteration step.

The total pair interaction energy [1] comprises the Van der Waals (U_v), elastic (U_e), and electrostatic (U_q) interparticle interactions: $U_{\text{tot}} = U_v + U_e + U_q(R_{ij}, t)$. Moreover, the modified Brownian dynamics model allows for the energy of electrostatic interaction between nanoparticles with charges $Z_i(x, t)$ and $Z_j(x, t)$ varying with time:

$$\begin{aligned} U_q(R_{ij}, t) &= \frac{Z_i^2 c_{jj} - 2Z_i Z_j c_{ij} + Z_j^2 c_{ii}}{2(c_{ii} c_{jj} - c_{ij}^2)} \\ &\quad - \frac{Z_i^2}{8\pi\epsilon\epsilon_0 R_i} - \frac{Z_j^2}{8\pi\epsilon\epsilon_0 R_j}. \end{aligned} \quad (14)$$

The first term in Eq. (14) corresponds to the energy of interaction between the charged particles with allowance for the electrical image forces (see [16]), whereas the two latter terms correspond to the intrinsic energies of the particles.

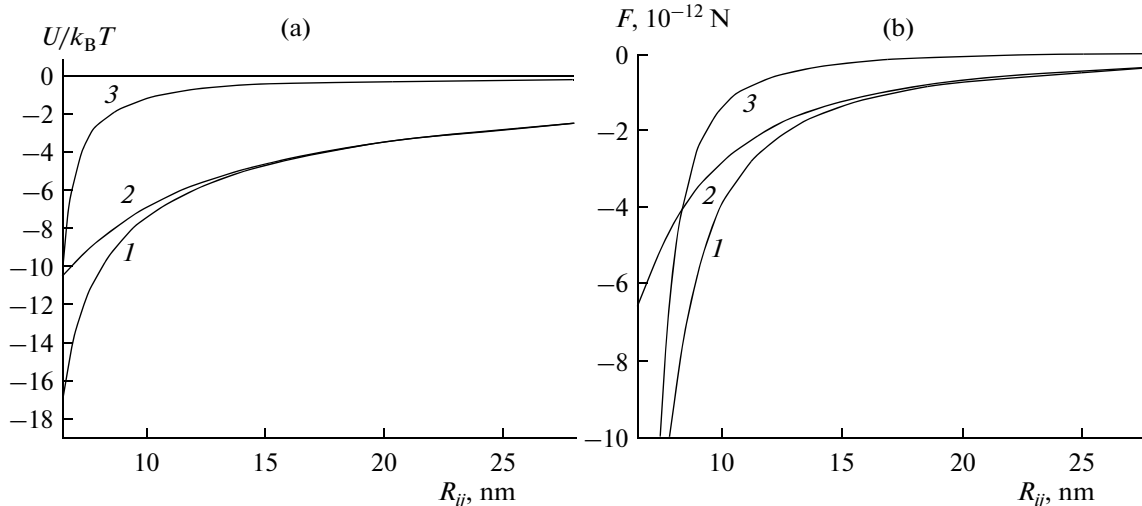


Fig. 3. Dependences of (a) energy and (b) force of pair interparticle interaction on intercenter distance R_{ij} for a pair with particle sizes $R_i = 1$ and $R_j = 5$ nm: the thickness of the adsorption layers is $h_i = h_j = 0.5$ nm: (1) electrostatic interaction with allowance for the contribution of electrical images, (2) Coulomb interaction, and (3) Van der Waals interaction ($T = 300$ K).

It should be noted that it is more reasonable to use the expression for the total energy of the electrostatic (with allowance for the image forces) interaction in the calculations than the equation for the Coulomb interaction. This circumstance can be explained by the fact that expression (14) more adequately describes the short-range component of the interaction between conducting particles of finite sizes with allowance for the image charges induced in them upon electron tunneling from an emitting particle to a neighboring one. This additional short-range component of the interaction obviously enhances the coagulation efficiency of the collisions.

As can be seen from Fig. 3a, the total energy of the electrostatic interaction in a pair of particles with radii of 1 and 5 nm is higher than the energy of the Coulomb and the Van der Waals interactions at interparticle distances corresponding to the area of the contact between the adsorption layers of the particles.

In particular, at a gap width of 0.5 nm (twofold deformation of the AL), the energy of the electrostatic pair interaction is equal to $-17k_B T$ ($T = 300$ K), whereas the Coulomb interaction energy is approximately $-10k_B T$. When the particle adsorption layers are in contact with one another (the interparticle gap is 1 nm), the energy of the interparticle electrostatic interaction is $-14k_B T$, while the Coulomb interaction energy value is $-9k_B T$.

The values of the electrostatic and Coulomb energies become equal at a gap width of approximately 5 nm. Thus, allowance for a more realistic electrostatic interaction between nanoparticles is a significant factor accelerating sol coagulation.

Figure 3b illustrates the dependence of the pair interaction forces on interparticle distance. The resultant of the forces is calculated at each iteration

step t with allowance for the total energy of pair interparticle interaction $U_{\text{tot}}(R_{ij}, t) = U_v(R_{ij}) + U_e(R_{ij}) + U_q(R_{ij}, t)$ for all pairs particles that comprise particle i under consideration.

3. RESULTS AND DISCUSSION

Bimodal ensembles composed of $N = 100$ silver nanoparticles with radii 2 and 4 or 1 and 5 nm were simulated. The thickness of the polymer adsorption layer for all particles was assumed to be $h_i = h_j = 0.5$ nm, and the characteristic values of the interparticle gap were $h = 0.5\text{--}0.8$ nm. Coagulation half-time $t_{1/2}$ was calculated as depending on the initial concentration v_0 of particles in an ensemble for two viscosity values of the dispersion medium ($\eta = 10^{-3}$ and 10^{-4} Pa s).

The dependences of the coagulation half-times on particle concentration $t_{1/2}(v_0)$ determined using the Brownian dynamics method for the viscosity of the dispersion medium corresponding to a hydrosol ($\eta = 10^{-3}$ Pa s) are shown in Fig. 4a. As can be seen from Fig. 4a, the allowance for ETE and the ETE-induced mutual heteropolar charging of particles with different sizes results in an approximately 20-fold acceleration in the coagulation of the bimodal ensembles as compared to the monodisperse ensemble of particles with a radius of 3 nm.

Analogous dependences plotted with no allowance for ETE [1] are shown in Fig. 4b for comparison. These dependences illustrate the violation of the “conventional” regularity for the coagulation of polydisperse colloids.

Figures 5a and 5b show the $t_{1/2}(v_0)$ dependences obtained for a dispersion medium with the viscosity value that is characteristic of certain organosols ($\eta =$

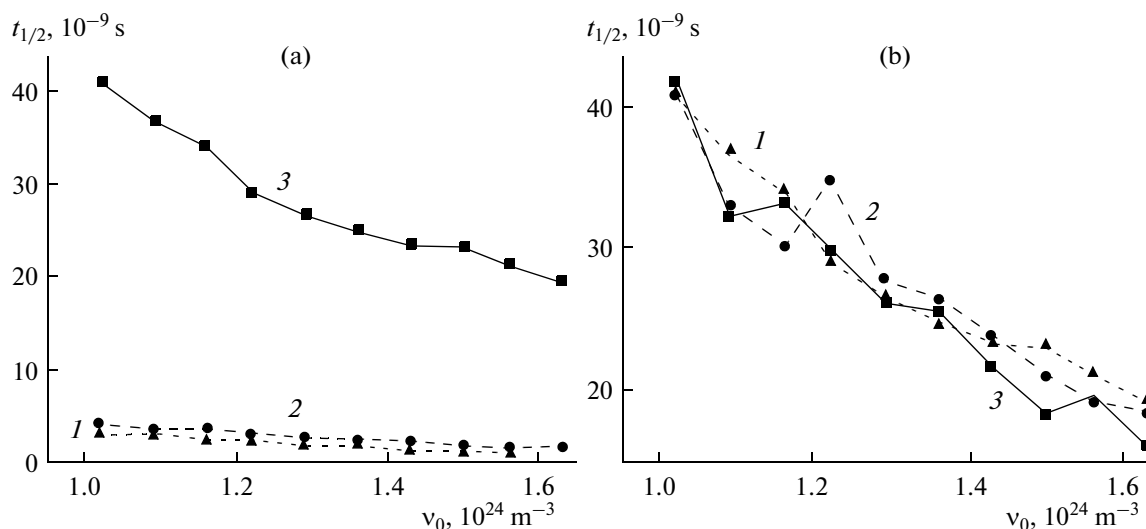


Fig. 4. Kinetic dependences of coagulation half-time $t_{1/2}$ on particle concentration for: (1) a bimodal ensemble with particle radii $R_i = 1$ and $R_j = 5$ nm, (2) a bimodal ensemble with particle radii $R_i = 2$ and $R_j = 4$ nm, and (3) a monodisperse ensemble with $R_i = 3$ nm. The calculations were performed (a) with and (b) without allowance for mutual particle charging (see Fig. 6a in [1]). The thickness of the polymer AL is $h_i = h_j = 0.5$ nm. Viscosity of the interparticle medium is $\eta = 10^{-3}$ Pa s. Particle number is $N = 100$.

10^{-4} Pa s). In this case, the aggregation rate of the bimodal colloid (Fig. 5a) with allowance for ETE is higher by almost an order of magnitude than that of the monodisperse ensemble.

An approximately twofold decrease in the aggregation rate at the lower viscosity of the interparticle medium, as compared to the medium with the higher viscosity ($\eta = 10^{-3}$ Pa s) (see the positions of curves 1 and 2 in Figs. 4a and 5a), is explained by partial disintegration of the aggregates being formed.

Figure 6 shows the $t_{1/2}(v_0)$ dependence for the ensembles with the Gaussian size distribution of particles (confined to the radius range of 1–5 nm), which is more natural for real disperse systems; the average particle radius is 3 nm, and the root-mean-square deviation is 2 nm. At the interparticle medium viscosity corresponding to water (hydrosol), $\eta = 10^{-3}$ Pa s, the effect of the mutual charging is found to accelerate the coagulation of the polydisperse ensemble by almost an order of magnitude, as compared to monodisperse systems (see Fig. 6a, curves 1, 3).

However, at $\eta = 10^{-4}$ Pa s (Fig. 6b), the mutual charging has a substantially weaker effect on the acceleration of the coagulation in the ensemble with the same degree of polydispersity (see curves 1, 2) because of the considerable disintegration of aggregates being formed.

CONCLUSIONS

The conditions under which the coagulation of metal nanocolloids can be accelerated with an increase in the degree of their polydispersity and the

conditions under which polydispersity has no effect on the coagulation kinetics have been established and analyzed in this study.

A physical model eliminating the controversy in the results obtained using the Brownian dynamics method and the conventional Muller–Smoluchowski theory for coagulation of polydisperse colloidal systems has been proposed.

It has been demonstrated that mutual heteropolar charging of particles with different sizes due to interparticle electron tunneling results in an additional interparticle electrostatic interaction (as compared with monodisperse systems). This phenomenon may considerably accelerate the coagulation of polydisperse metal nanocolloids. Using the example of silver colloids and using the Brownian dynamics method, it has been demonstrated that the effect of mutual heteropolar particle charging changes the interparticle potential and accelerates the coagulation in ensembles of polydisperse nanoparticles by more than an order of magnitude. It should be emphasized that the proposed model is primarily applicable to systems containing no free electric charges in dispersion medium, because the adsorption of these charges can neutralize the intrinsic particle charge resulting from the mutual charging.

The results obtained suggest that it is necessary to modify the models of polydisperse metal sol coagulation with regard to the electron tunneling effect and mutual heteropolar particle charging. It is noteworthy that this effect can take place not only when the work function depends on the particle size, but also for het-

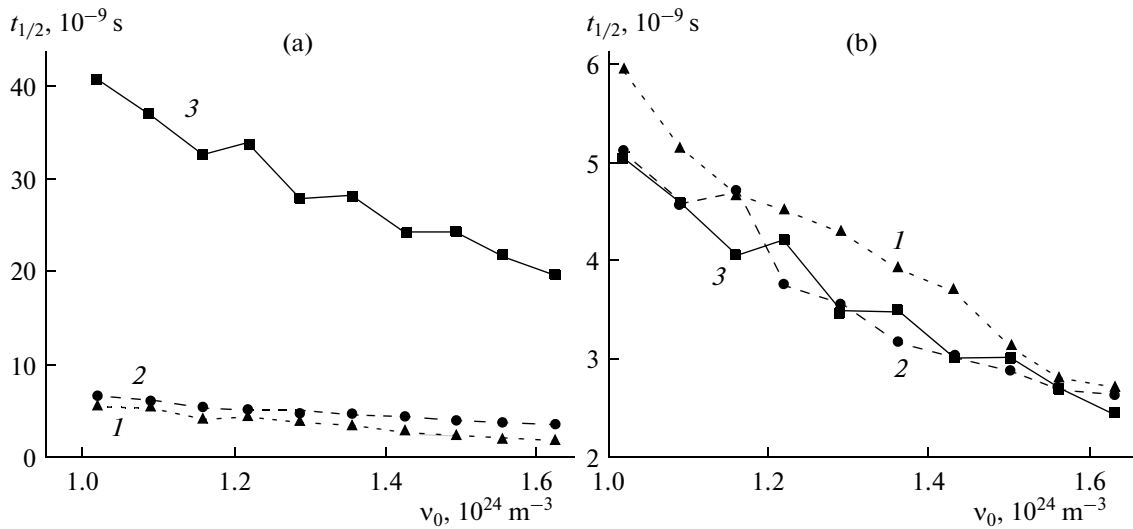


Fig. 5. Kinetic dependences of coagulation half-time $t_{1/2}$ on particle concentration for: (1) a bimodal ensemble with particle radii $R_i = 1$ and $R_j = 5$ nm, (2) a bimodal ensemble with particle radii $R_i = 2$ and $R_j = 4$ nm, and (3) a monodisperse ensemble with $R_i = 3$ nm. The calculations were performed (a) with and (b) without allowance for mutual particle charging (see Fig. 6b in [1]). The thickness of the polymer AL is $h_i = h_j = 0.5$ nm. Viscosity of the interparticle medium is $\eta = 10^{-4}$ Pa s. Particle number is $N = 100$.

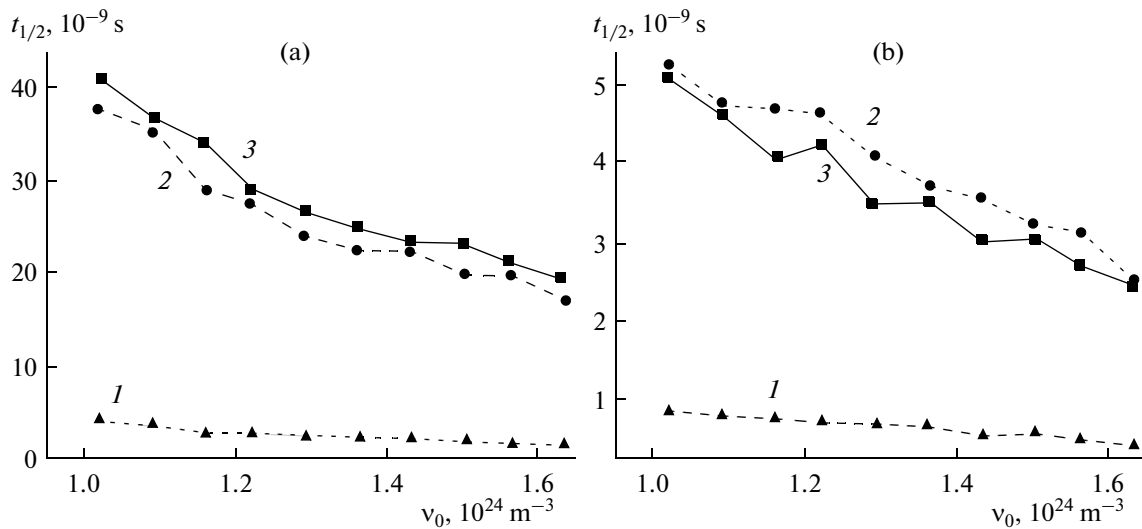


Fig. 6. The kinetic dependences of coagulation half-time $t_{1/2}$ on particle concentration v_0 for a polydisperse ensemble with the Gaussian particle size distribution (dispersion $\sigma = 2$ nm) (1) with and (2) without allowance for the electron tunneling effect and (3) for a monodisperse sol with $R_i = 3$ nm. Viscosity of the medium is $\eta =$ (a) 10^{-3} and (b) 10^{-4} Pa s. The thickness of the polymer AL is $h_i = h_j = 0.5$ nm. Particle number is $N = 100$.

erocolloids (heterosols), in which the work function is determined by both the size and material of particles.

ACKNOWLEDGMENTS

Authors are thankful to G.A. Chiganova for discussions and helpful comments. Studies were carried out with the support of grants: the Presidium of RAS № 29

and № 31, OFN RAS III.9.5, IP SB RAS № 43, IP SB RAS (and SFU) № 101.

REFERENCES

1. Karpov, S.V. and Semina, P.N., *Kolloidn. Zh.*, 201, vol. 74, p. 329.
2. Voyutskii, S.S., *Kurs kolloidnoi khimii* (Colloid Chemistry), Moscow: Khimiya, 1975.

3. Myuller, G., *Teoriya koagulyatsii polidispersnykh sistem. Koagulyatsiya kolloidov* (TRANSLATION), Moscow: Glavn. Red. Khim. Lit., 1936.
4. Khachatryan, A.A. and Lunina, M.A., *Kolloidn. Zh.*, 1985, vol. 47, p. 562.
5. Lunina, M.A., Romina, N.N., and Korenev, A.D., *Kolloidn. Zh.*, 1989, vol. 51, p. 774.
6. Borzyak, P.G., Gorban', S.A., Grigor'eva, L.K., Nagaev, E.L., Nepiiko, S.A., and Chizhik, S.P., *Zh. Eksp. Teor. Fiz.*, 1990, vol. 97, p. 623.
7. Grigor'eva, L.K., Lidorenko, N.S., Nagaev, E.L., and Chizhik, S.P., *Pis'ma Zh. Eksp. Teor. Fiz.*, 1986, vol. 43, p. 290.
8. Nagaev, E.L., *Usp. Fiz. Nauk*, 1992, vol. 162, no. 9, p. 49.
9. Karpov, S.V., Isaev, I.L., Gavriilyuk, A.P., and Grachev, A.S., *Kolloidn. Zh.*, 2009, vol. 71, p. 347.
10. Kiely, C.J., Fink, J., Brust, M., Bethell, D., and Shiffrin, D.J., *Nature* (London), 1998, vol. 396, p. 444.
11. Kiely, C.J., Fink, J., Jian Guo Zheng, Brust, M., Bethell, D., and Shiffrin, D., J., *Adv. Mater.* (Weinheim, Fed. Repub. Ger.), 2000, vol. 12, p. 640.
12. Roldughin, V.I., *Usp. Khim.*, 2004, vol. 73, p. 123.
13. Blokhintsev, D.I., *Osnovy kvantovoi mekhaniki* (Fundamentals of Quantum Mechanics), Moscow: Nauka, 1976.
14. Landau, L.D. and Lifshits, E.M., *Elektrodinamika sploshnykh sred* (Electrodynamics of Continuous Media), Moscow: Nauka, 1982.
15. Nagaev, E.L., *Fiz. Tverd. Tela* (Leningrad), 1983, vol. 25, p. 1439.
16. Saranin, V.A., *Usp. Fiz. Nauk*, 1999, vol. 169, no. 4, p. 453.